Distinct combinations of variant ionotropic glutamate receptors mediate thermosensation and hygrosensation in *Drosophila*

Zachary A. Knecht[1,§], Ana F. Silbering[2,§], Lina Ni[1,§], Mason Klein[3,4 §], Gonzalo Budelli[1], Rati Bell[2], Liliane Abuin[2], Anggie J. Ferrer[4], Aravinthan D.T. Samuel[3]†, Richard Benton[2]†, and Paul A. Garrity[1]†

[1]National Center for Behavioral Genomics and Volen Center for Complex Systems Department of Biology, Brandeis University, Waltham, MA 02458, USA; [2]Center for Integrative Genomics, Faculty of Biology and Medicine, University of Lausanne, Lausanne CH-1015, Switzerland. [3]Department of Physics and Center for Brain Science, Harvard University, Cambridge, MA 02138; [4]Department of Physics, University of Miami, Coral Gables, FL 33146, USA.

§ equal contribution

† co-corresponding authors: Aravinthan Samuel, samuel@physics.harvard.edu, Richard Benton, Richard.Benton@unil.ch, and Paul Garrity, pgarrity@brandeis.edu

Communicating author:

Paul A. Garrity

National Center for Behavioral Genomics, Volen Center for Complex Systems Biology Department, Brandeis University MS-008,

415 South Street, Waltham, MA 02454.

E-mail: pgarrity@brandeis.edu;

Telephone: 781-736-3127; FAX: 781-736-8161

Author contributions: Z.A.K., A.F.S., L.N., M.K., G.B., A.D.T.S., R. Benton, and P.A.G. designed experiments. Z.A.K. performed molecular genetics, behavior, immunohistochemistry and data analysis, A.F.S. performed neurophysiology, immunohistochemistry and data analysis, L.N. performed molecular genetics, neurophysiology, behavior, immunohistochemistry and data analysis, M.K. performed neurophysiology, behavior and data analysis, G.B. performed neurophysiology, R. Bell performed molecular genetics, L.A. performed immunohistochemistry; A.J.F. performed data analysis, Z.A.K., R. Benton and P.A.G. wrote the paper with contributions from all authors.

Abstract: Ionotropic Receptors (IRs) are a large subfamily of variant ionotropic glutamate receptors present across Protostomia. While these receptors are most extensively studied for their roles in chemosensory detection in insects, recent work has implicated two family members, IR21a and IR25a, in thermosensation in *Drosophila*. Here we characterize one of the most deeply conserved receptors, IR93a, and show that it is co-expressed and functions with IR21a and IR25a to mediate physiological and behavioral responses to cool temperatures. IR93a is also co-expressed with IR25a and a distinct receptor, IR40a, in a discrete population of sensory neurons in the sacculus, a multi-chambered pocket within the antenna. We demonstrate that this combination of receptors is important for neuronal responses to dry air and behavioral discrimination of humidity differences. Our results identify IR93a as a common component of molecularly and cellularly distinct IR pathways underlying thermosensation and hygrosensation in insects.

INTRODUCTION:

Ionotropic Receptors (IRs) are a large subfamily of ionotropic glutamate receptors (iGluRs) that evolved in the last common protostome ancestor (Benton et al., 2009; Croset et al., 2010; Rytz et al., 2013). In contrast to the critical role of iGluRs in synaptic communication, IRs have diverse roles in chemosensory detection (Koh et al., 2014; Rytz et al., 2013). The best-defined functions of IRs are in olfaction, where they mediate odor-evoked sensory neuron responses to diverse chemicals, including many acids and amines (Rytz et al., 2013; Silbering et al., 2011). Most IRs are thought to form heteromeric ligand-gated ion channels, in which broadly expressed co-receptor subunits (e.g., IR8a, IR25a and IR76b) combine with more selectively expressed IR subunits that confer stimulus specificity (Abuin et al., 2011; Rytz et al., 2013). Many of these IRs are deeply conserved in insects, indicating that they define sensory pathways common to a wide range of species (Croset et al., 2010; Rytz et al., 2013).

Although most conserved IRs have been assigned chemosensory roles, we recently reported that one of these receptors, IR21a, mediates cool sensing (together with IR25a), in a population of neurons in the *Drosophila melanogaster* larva, the dorsal organ cool cells (DOCCs) (Ni et al., 2016). This finding raised the possibility that other IRs serve non-chemosensory functions. In this work we characterize one of the most deeply conserved “orphan” receptors, IR93a, which has orthologous genes across arthropods (Corey et al., 2013; Groh-Lunow et al., 2014; Rytz et al., 2013). RNA expression analysis in several insects and crustaceans indicate that this receptor gene is transcribed in peripheral sensory organs (Benton et al., 2009; Corey et al., 2013; Groh-Lunow et al., 2014; Rytz et al., 2013), but its role(s) are unknown. Using

Drosophila as a model, we find that IR93a acts in combination with distinct sets of IRs in different populations of neurons to mediate physiological and behavioral responses to both thermosensory and hygrosensory cues.

RESULTS

IR93a is expressed in larval thermosensory neurons and is essential for cool avoidance

To investigate the expression and function of IR93a, we generated antibodies against a C-terminal peptide sequence of this receptor, and obtained two *Ir93a* mutant alleles: $Ir93a^{MI05555}$, which contains a transposon insertion in the fifth coding exon, and $Ir93a^{122}$, which we generated using CRISPR/Cas9 to delete 22 bases within sequences encoding the first transmembrane domain (Figure 1a).

In larvae, IR93a protein is expressed in several neurons in the dorsal organ ganglion, one of the main sensory organs in the larval head (Stocker, 1994) (Figure 1b-c). These neurons encompass the DOCCs (labeled by an *Ir21a promoter-Gal4*-driven GFP reporter), and the protein localizes prominently to the dendritic bulb at the tip of the sensory processes of these cells (Figure 1c). All expression was absent in *Ir93a* mutants, confirming antiserum specificity (Figure 1c).

These observations indicated that IR93a might function in cool sensing. Indeed, when larval thermotaxis was assessed on a thermal gradient (Klein et al., 2015), we found both *Ir93a* mutant alleles exhibit strong defects in cool avoidance (Figure 1d). Cell-specific expression of an *Ir93a* cDNA in the DOCCs under *Ir21a-Gal4* control fully

rescued this mutant phenotype (Figure 1d). These data demonstrate an essential role for IR93a in DOCCs in larval thermotaxis.

IR93a is required, together with IR21a and IR25a, for cool-dependent physiological responses of DOCCs

We next assessed whether IR93a is required for the physiological responses of DOCCs to cooling by optical imaging of these neurons using the genetically encoded calcium indicator, GCaMP6m (Chen et al., 2013). As previously reported (Klein et al., 2015; Ni et al., 2016), wild-type DOCCs exhibit robust increases in intracellular calcium in response to cooling (Figure 2a). These responses were dramatically reduced in *Ir93a* mutants, and could be rescued by cell-specific expression of an *Ir93a* cDNA (using the *R11F02-Gal4* DOCC driver (Klein et al., 2015)) (Figure 2a). This dramatic loss of DOCC temperature sensitivity resembles that observed in both *Ir21a* and *Ir25a* mutants (Ni et al., 2016), and is consistent with IR21a, IR25a and IR93a functioning together to mediate cool activation of the DOCCs.

To provide a more direct readout of thermotransduction in these neurons than soma calcium measurements, we tested the requirement for IR93a, IR21a and IR25a in cool-evoked membrane voltage changes using the genetically encoded voltage sensor, Arclight (Jin et al., 2012). In wild-type animals, cool-dependent voltage changes were observed in the DOCC sensory dendritic bulbs (Figure 2c-d), where IRs are localized (Figure 1c). This response was completely eliminated in *Ir21a*, *Ir25a* and *Ir93a* mutants (Figure 2c-e), indicating that each of these IRs is required for temperature-dependent voltage changes in this sensory compartment.

IR93a is co-expressed with IR25a and IR40a in the antennal sacculus

In adults, *Ir93a* transcripts were previously weakly detected in a set of neurons in the third antennal segment surrounding the sacculus, a three-chambered pouch whose opening lies on the posterior surface of the antenna (Benton et al., 2009) (Figure 3a). With our IR93a antibody, we detected IR93a expression in neurons innervating sacculus chamber I (11.0±0.5 neurons, n=48 animals; mean ± SEM) and chamber II (13.9±0.7, n=23), with signal detected both in the soma and in the sensory cilia that project into cuticular sensory hairs (sensilla) (Figure 3b). By contrast, while IR25a is expressed in IR93a-expressing cells in the sacculus (Figure 3c), neither *Ir21a* transcripts nor *Ir21a* promoter drivers were detected in these cells ((Benton et al., 2009) and data not shown). The IR93a sacculus neurons express instead a distinct receptor, IR40a (Figure 3d) (Benton et al., 2009; Silbering et al., 2016). IR40a does not appear to be expressed in the larval DOCCs (data not shown), suggesting that these sacculus cells have another sensory function.

IR93a, IR25a and IR40a are necessary for hygrosensory behavior

Morphological studies have suggested that neurons in sacculus chambers I and II are hygroreceptive (Shanbhag et al., 1995), raising the possibility that IR93a, IR25a, and IR40a are required for hygrosensory behaviors. To test this hypothesis, we adapted an experimental paradigm (Perttunen and Salmi, 1956) in which flies choose between regions of differing humidity generated by two underlying chambers: one containing deionized water and the other containing water saturated with a non-volatile solute

(ammonium nitrate) to lower its vapor pressure (Figure 4a). This assay design created a humidity gradient of ~96% relative humidity (RH) to ~67% RH, with negligible variation in temperature (Figure 4b). Consistent with previous observations (Perttunen and Salmi, 1956), wild-type flies exhibited a strong preferences for lower humidity (Figure 4c). This preference was completely eliminated in *Ir93a* and *Ir25a* mutant flies, and significantly reduced, but not abolished, in *Ir40a* mutants (Figure 4c). All of these behavioral defects were robustly rescued by the corresponding cDNAs, confirming the specificity of the mutant defects (Figure 4c). Importantly, the loss of *Ir21a* (or other antennal-expressed IR co-receptors, *Ir8a* and *Ir76b*) did not disrupt dry preference. To exclude any potential contribution of the non-volatile solute to the behavior observed, we also tested flies in a humidity gradient (~89% to ~96% RH) generated using underlying chambers of deionized water alone and air (Figure 4a). Even in this very shallow gradient, wild type flies displayed a strong preference for lower humidity (Figure 4d), which was dependent IR93a, IR25a and IR40a, but independent of IR21a (Figure 4d). This distinction between the functions of IR21a and IR40a extended to thermotaxis, as *Ir40a* mutants exhibited no defects in this IR21a-dependent behavior (Figure 4 – supplement 1b).

IRs mediate dry detection by sacculus neurons

To test whether the IR40a/IR93a/IR25a-expressing sacculus neurons are physiological hygrosensors, we monitored their calcium responses to changes in the RH of an airstream (of constant temperature) directed towards the antenna. We used *Ir40a-Gal4* to express *UAS-GCaMP6m* selectively in these neurons, and measured GCaMP6m

fluorescence in their axon termini, which innervate two regions of the antennal lobe, the "arm" and the "column" (Silbering et al., 2016; Silbering et al., 2011) (Figure 5a-b).

We observed that these sacculus neurons behave as dry-activated hygrosensors: decreasing the RH from ~90% to ~7% RH elicited an increase in GCaMP6m fluorescence, while increasing RH from ~7% to ~90% elicited a decrease (Figure 5c-g). Calcium changes were most apparent in the "arm" (Figure 5c). Importantly, these physiological responses are IR-dependent: mutations in either *Ir93a* or *Ir40a* eliminated the dry response (*Ir25a* mutants were not tested), and these defects were restored with corresponding cDNA rescue transgenes (Figure 5d-g). These data corroborate the requirement for IRs in behavioral preference for lower humidity.

DISCUSSION:

From their ancestral origins within the synaptic iGluR family, IRs are widely appreciated to have evolved functionally diverse roles in environmental chemosensory detection (Croset et al., 2010; Rytz et al., 2013). Here we provide evidence that a previously uncharacterized member of this repertoire, IR93a, functions in two critical non-chemosensory modalities, thermosensation and hygrosensation. In both of these roles, IR93a acts with the broadly expressed co-receptor IR25a. However, IR93a mediates these two modalities in different populations of neurons in conjunction with a third, distinct IR: with IR21a in cool sensation, but not dry sensation, and with IR40a in dry sensation, but not cool sensation. All of these receptors are deeply conserved in insects, indicating that these sensory pathways likely underlie behavioral responses of diverse species to these important environmental stimuli. This conservation also

suggests that the non-chemosensory roles of IRs could be as ancient as the receptor family itself.

The identification of an IR21a/IR25a/IR93a-dependent cool-sensing system provides a molecular counterpart to the well-established Transient Receptor Potential (TRP) (Barbagallo and Garrity, 2015), and Gustatory Receptor GR28B(D) (Ni et al., 2013) warmth-sensing systems. By contrast, despite the importance of hygrosensation in helping insects to avoid desiccation or inundation (Chown et al., 2011) and – in blood-feeding disease vectors such as mosquitoes – to locate mammalian hosts (Brown, 1966; Olanga et al., 2010), the neuronal and molecular basis of this sensory modality has been largely mysterious. Hygrosensitive neurons have been identified electrophysiologically in large insects (Tichy and Gingl, 2001; Tichy and Kallina, 2010), but their behavioral relevance has been hard to determine. In *Drosophila*, the antenna has long been suspected to be an important hygrosensory organ (Perttunen and Syrjamaki, 1958; Sayeed and Benzer, 1996), but there has been little consensus on the relevant populations of neurons and sensory receptors (Ji and Zhu, 2015; Liu et al., 2007; Yao et al., 2005). The TRP channels Nanchung and Waterwitch have been suggested to contribute to hygrosensory behavior in *Drosophila* (Liu et al., 2007), but these appear to be broadly expressed in the antenna, and there has been no direct physiological analysis of the cells expressing these channels. Our characterization of IR40a/IR93a/IR25a-expressing sacculus neurons, together with data from an independent study (Enjin et al., 2016), provide physiological and behavioral evidence supporting these as one pathway that enables flies to distinguish external humidity levels.

In addition to the roles of IR93a in cool and dry sensing, it is very likely that this receptor defines additional sensory pathways. Our expression analysis has identified IR93a-positive cells that do not express IR21a or IR40a, such as non-DOCCs in the larval dorsal organ (Figure 1c). Moreover, the milder hygrosensory behavior phenotype of our protein null *Ir40a* mutants compared to *Ir93a* (or *Ir25a*) mutants hints that IR93a may have broader roles in this sensory modality than acting exclusively with IR40a. Finally, we suspect that the populations of IR93a-expressing neurons characterized in this study are themselves functionally heterogeneous. For example, IR40a/IR93a-expressing sacculus neurons appear to belong to two morphologically and physiologically distinct subpopulations: “arm” neurons respond preferentially to low humidity, while “column” neurons display preferential response to chemical stimuli (Silbering et al., 2016). The molecular and/or cellular basis for this heterogeneity is not yet known, but is reminiscent of the distinct subpopulations of IR64a-expressing neurons in sacculus chamber III (Ai et al., 2013; Ai et al., 2010).

A key future challenge will be to determine the mechanism by which IRs sense thermal and humidity cues. As IR21a and IR40a may be specificity determinants, it will be of particular interest to determine the contribution (if any) of their Venus flytrap-like “ligand-binding” domain (which recognizes glutamate in iGluRs, and diverse organic molecules in chemosensory IRs). The requirement for IR93a (and IR25a) in these distinct sensory modalities also indicates that they might share common mechanisms of sensory detection. For example, hygrosensation could involve a thermosensory component, based on evaporative cooling. Alternatively, both temperature and moisture detection could involve mechanosensation, based on swelling or shrinkage of sensory

structures. Such mechanisms have been suggested to underlie hygrosensation in mammals and *C. elegans* (Filingeri, 2015; Russell et al., 2014), and may explain why hygrosensors in *Drosophila* are located in the morphologically highly-specialized sacculus. Further characterization of how IRs mediate temperature and moisture detection is currently hampered by our inability to reconstitute IR-based thermosensory or hygrosensory responses in heterologous expression systems through expression of the known combinations of IRs (G.B., L.N., A.F.S., R.B. and P.G., unpublished data). These observations imply the existence of additional molecules and/or specialized cellular structures that permit sensory detection of these ubiquitous and ever-changing environmental stimuli.

Material and Methods:

Fly strains. *Ir25a*^{2} (Benton et al., 2009), *UAS-Ir25a* (Abuin et al., 2011), *Ir8a*^{1} (Abuin et al., 2011), *Ir21a*^{123} (Ni et al., 2016), *Ir76b*^{2} (Zhang et al., 2013), *R11F02-Gal4* (Klein et al., 2015), *Ir40a-Gal4* (Silbering et al., 2011), *Ir40a*^{1} (Silbering et al., 2016), *UAS-Ir40a* (Silbering et al., 2016), *Ir93a*^{MI05555} (Venken et al., 2011), *UAS-GCaMP6m* (*P[20XUAS-IVS-GCaMP6m]attp2* and *P[20XUAS-IVS-GCaMP6m]attp2attP40* (Chen et al., 2013)), *UAS-Arclight* (Cao et al., 2013), *UAS-GFP* (*P[10XUAS-IVS-Syn21-GFP-p10]attP2* (Pfeiffer et al., 2012)), and *y1 P(act5c-cas9, w+) M(3xP3-RFP.attP)ZH-2A w** (Port et al., 2014).

Ir40a^{134} (Figure 4 supplement 1a) and *Ir93a*^{122} (Figure 1a) were generated by transgene-based CRISPR/Cas9-mediated genome engineering as described (Port et al., 2014), using either an *Ir40a*-targeting gRNA (5'-GCCCGTTTAAGCAAGACATC) or

an *Ir93a*-targeting gRNA (5'-TCAGCAGAATGATGCCCATT) expressed under U6-3 promoter control (dU6-3:gRNA) in the presence of *act-cas9* (Port et al., 2014). *UAS-mCherry:Ir93a* contains codons 29-869 of the *Ir93a* ORF (corresponding to *Ir93a-PD* [flybase.org], without the sequence encoding the predicted endogenous signal peptide), which were PCR amplified from Oregon R antennal cDNA and subcloned into *pUAST-mCherry attB* (Abuin et al., 2011) (which encodes the calreticulin signal sequence upstream of the *mCherry* ORF). This construct was integrated into VK00027 by phiC31-mediated transgenesis (Genetic Services, Inc.).

Behavior. Thermotaxis of early second instar larvae was assessed over a 15 min period on a temperature gradient extending from 13.5 to 21.5°C over 22 cm (~0.36 ˚C/cm) as described (Klein et al., 2015). As thermotaxis data were normally distributed (as assessed by Shapiro-Wilk test), statistical comparisons were performed by Tukey HSD test, which corrects for multiple comparisons.

To assay hygrosensory behavior, 8 well rectangular dishes (12.8 x 8.55 x 1.5 cm; ThermoFisher #267060) were modified to serve as humidity preference chambers. The lids of two 8 well plates were used. A heated razor blade was used to cut out the middle of one lid, and a nylon mesh was glued into place around the edges, providing a surface for the animals to walk on which separated them from contact with any liquid. A soldering iron was used to melt a small hole in a second culture plate lid, which could then be placed over the screen, creating a chamber ~0.7 cm in height in which the flies could move freely. To monitor the gradients formed, an additional chamber was constructed with four holes equally spaced along its length to allow the insertion of

277 humidity sensors (Sensirion EK-H4 evaluation kit) for monitoring the humidity and
278 temperature.

279 Prior to the start of each experiment, 4 wells on one side of the culture dish were
280 filled with purified water, while the opposite 4 were filled with ~4 ml water and sufficient
281 ammonium nitrate to obtain a saturated solution (~3 g). The gradient was assembled
282 with the screen and lid piece, and the whole apparatus wrapped in food service film to
283 avoid any transfer of air between the inside and outside of the device. Gradients were
284 transferred to an environmental room that maintained at constant external temperature
285 and humidity (25˚C and 70%RH). Ammonium nitrate gradients were permitted to
286 equilibrate for approximately 1 hour and were stable over many hours. For the water
287 and air only gradients, the air only side humidified over time. These gradients were
288 incubated for 25 minutes prior to use to allow the temperature to equilibrate; the
289 humidity of the dry side typically rose by ~2% RH during the 30 minute assay (values
290 shown are at the 30 minute time point). A small hole was poked through the food
291 service film covering the device to allow animals to be transferred to the gradient. This
292 hole was sealed using transparent scotch tape once the animals were inside.
293 Experiments used 1-4 day old adult flies that had been sorted under light CO2
294 anesthesia into groups of 30 (15 male and 15 female) animals 24 hours before testing,
295 and transferred to fresh tubes. Flies were allowed 30 minutes to settle on the gradient,
296 at which point a photograph was taken of their position, and the number of animals on
297 each side counted, allowing calculation of a dry preference index as follows:

$$\text{Dry Preference} = \frac{\text{\# animals on dry side - \# animals on moist side}}{\text{total \# of animals}}$$

As moisture preference data did not conform to normal distributions (as assessed by Shapiro-Wilk test, $p<0.01$), statistical comparisons to wild-type control were performed by Steel test, a non-parametric test that corrects for multiple comparisons, using JMP11 (SAS).

Calcium and Arclight imaging. Calcium and Arclight imaging of larval thermosensors was performed as previously described (Klein et al., 2015). Pseudocolor images were created using the 16_colors lookup table in ImageJ 1.43r. Adult antennal lobe calcium imaging was performed as described for olfactory imaging (Silbering et al., 2012), with slight modifications to sample preparation and stimulation. Briefly, 3-7 day old flies were fixed to a Plexiglas stage using UV-glue (A1 Tetric Evoflow, Ivoclar Vivadent), the antennae were pulled forward and a small opening was made in the head capsule to allow visual access to the antennal lobes. For the stimulation compressed air from a tank was passed through activated charcoal and then either through an empty gas washing bottle or a gas washing bottle filled with distilled water producing either a dry airstream of ~7%RH or a humid airstream of ~90%RH. A computer controlled solenoid valve (The Lee Company, Westbrook, CT, USA) was used to switch the airflow between the two gas washing bottles. The flow was kept constant at 1 l/min with a parallel arrangement of two 500ml/min Mass Flow controllers (PKM SA, www.pkmsa.ch) placed before the gas washing bottles. Activating the solenoid valve resulted in a complete reversal of RH from low to high or high to low within less than 10 seconds. For each animal tested, both high to low and low to high RH transitions were applied in random order. Following humidity stimulation, a final pulse of 10% ammonia was applied as a

control to confirm cellular activity (Silbering et al., 2016) (animals showing no response to this positive control were excluded from the analysis). Data were processed using Stackreg (ImageJ) (Thevenaz et al., 1998) to correct for movement artifacts (animals with movement artifacts that could not be corrected with Stackreg were excluded from the analysis) and custom scripts in Matlab and R as previously described (Silbering et al., 2011). As quantified imaging data did not conform to normal distributions (as assessed by Shapiro-Wilk test, $p<0.01$), statistical comparisons were performed by Steel-Dwass test, a non-parametric test that corrects for multiple comparisons, using JMP11 (SAS).

Immunohistochemistry. Larval immunostaining was performed as described (Kang et al., 2012). Immunofluorescence on antennal cryosections or whole-mount antennae was performed essentially as described (Saina and Benton, 2013), except that whole-mount antennae were placed in Vectashield immediately after the final washes without dehydration. The following antibodies were used: rabbit anti-IR25a (1:1000; (Benton et al., 2009)), guinea pig anti-IR40a (1:200, (Silbering et al., 2016)), rabbit anti-IR93a (peptide immunogen CGEFWYRRFRASRKRRQFTN, Proteintech, Rosemont, IL, USA, 1:4000 for tissue sections and 1:500 for whole-mount tissue), guinea pig anti-IR25a (peptide immunogen SKAALRPRFNQYPATFKPRF, Proteintech, Rosemont, IL, USA, 1:200), mouse anti-GFP (1:200; Roche), goat anti-rabbit Cy3 (1:100 larva, 1:1000 sections; Jackson ImmunoResearch), goat anti-rabbit Alexa488 (1:100 antenna whole-mount, 1:1000 antennal sections, A11034 Invitrogen AG), goat anti-guinea pig (1:1000,

A11073 Invitrogen AG) and donkey anti-mouse FITC (1:100; Jackson ImmunoResearch).

Acknowledgements:

This work was supported by a grant from the National Institute on Deafness and Other Communication Disorders (F31 DC015155) to Z.A.K., the National Institute of Neurological Disorders and Stroke (F32 NS077835) to M.K., a Boehringer Ingelheim Fonds PhD Fellowship to R. Bell, European Research Council Starting Independent Researcher and Consolidator Grants (205202 and 615094) and a Swiss National Science Foundation Project Grant (31003A_140869) to R. Benton, the National Institute of General Medical Science (F32 GM113318) to G.B., and the National Institute of General Medical Sciences (P01 GM103770) to A.D.T.S. and P.A.G.

Competing interests: The authors have no competing interests.

References

Abuin, L., Bargeton, B., Ulbrich, M.H., Isacoff, E.Y., Kellenberger, S., and Benton, R. (2011). Functional architecture of olfactory ionotropic glutamate receptors. Neuron *69*, 44-60. doi: 10.1016/j.neuron.2010.11.042

Ai, M., Blais, S., Park, J.Y., Min, S., Neubert, T.A., and Suh, G.S. (2013). Ionotropic glutamate receptors IR64a and IR8a form a functional odorant receptor complex in vivo in Drosophila. J Neurosci *33*, 10741-10749. doi: 10.1523/JNEUROSCI.5419-12.2013

Ai, M., Min, S., Grosjean, Y., Leblanc, C., Bell, R., Benton, R., and Suh, G.S. (2010). Acid sensing by the Drosophila olfactory system. Nature *468*, 691-695. doi: 10.1038/nature09537

Barbagallo, B., and Garrity, P.A. (2015). Temperature sensation in Drosophila. Current opinion in neurobiology *34C*, 8-13. doi: 10.1016/j.conb.2015.01.002

Benton, R., Vannice, K.S., Gomez-Diaz, C., and Vosshall, L.B. (2009). Variant ionotropic glutamate receptors as chemosensory receptors in Drosophila. Cell *136*, 149-162.

Brown, A.W.A. (1966). The attraction of mosquitoes to hosts. Journal of the American Medical Association *196*, 159-162.

Cao, G., Platisa, J., Pieribone, V.A., Raccuglia, D., Kunst, M., and Nitabach, M.N. (2013). Genetically targeted optical electrophysiology in intact neural circuits. Cell *154*, 904-913. doi: 10.1016/j.cell.2013.07.027

Chen, T.W., Wardill, T.J., Sun, Y., Pulver, S.R., Renninger, S.L., Baohan, A., Schreiter, E.R., Kerr, R.A., Orger, M.B., Jayaraman, V., Looger, L.L., Svoboda, K., and Kim, D.S. (2013). Ultrasensitive fluorescent proteins for imaging neuronal activity. Nature *499*, 295-300. doi: 10.1038/nature12354

Chown, S.L., Sorensen, J.G., and Terblanche, J.S. (2011). Water loss in insects: an environmental change perspective. Journal of insect physiology *57*, 1070-1084. doi: 10.1016/j.jinsphys.2011.05.004

Corey, E.A., Bobkov, Y., Ukhanov, K., and Ache, B.W. (2013). Ionotropic crustacean olfactory receptors. PloS one *8*, e60551. doi: 10.1371/journal.pone.0060551

Croset, V., Rytz, R., Cummins, S.F., Budd, A., Brawand, D., Kaessmann, H., Gibson, T.J., and Benton, R. (2010). Ancient protostome origin of chemosensory ionotropic glutamate receptors and the evolution of insect taste and olfaction. PLoS genetics *6*, e1001064. doi: 10.1371/journal.pgen.1001064

Enjin, A., Zaharieva, E.E., Frank, D.D., Mansourian, S., Suh, G.S., Gallio, M., and Stensmyr, M.C. (2016). Humidity sensing in Drosophila. Current Biology *in press*.

Filingeri, D. (2015). Humidity sensation, cockroaches, worms, and humans: are common sensory mechanisms for hygrosensation shared across species? Journal of neurophysiology *114*, 763-767. doi: 10.1152/jn.00730.2014

Groh-Lunow, K.C., Getahun, M.N., Grosse-Wilde, E., and Hansson, B.S. (2014). Expression of ionotropic receptors in terrestrial hermit crab's olfactory sensory neurons. Frontiers in cellular neuroscience *8*, 448. doi: 10.3389/fncel.2014.00448

401 Ji, F., and Zhu, Y. (2015). A novel assay reveals hygrotactic behavior in Drosophila.
402 PloS one *10*, e0119162. doi: 10.1371/journal.pone.0119162

403 Jin, L., Han, Z., Platisa, J., Wooltorton, J.R., Cohen, L.B., and Pieribone, V.A. (2012).
404 Single action potentials and subthreshold electrical events imaged in neurons with a
405 fluorescent protein voltage probe. Neuron *75*, 779-785. doi:
406 10.1016/j.neuron.2012.06.040

407 Kang, K., Panzano, V.C., Chang, E.C., Ni, L., Dainis, A.M., Jenkins, A.M., Regna, K.,
408 Muskavitch, M.A., and Garrity, P.A. (2012). Modulation of TRPA1 thermal sensitivity
409 enables sensory discrimination in Drosophila. Nature *481*, 76-80. doi:
410 10.1038/nature10715

411 Klein, M., Afonso, B., Vonner, A.J., Hernandez-Nunez, L., Berck, M., Tabone, C.J.,
412 Kane, E.A., Pieribone, V.A., Nitabach, M.N., Cardona, A., Zlatic, M., Sprecher, S.G.,
413 Gershow, M., Garrity, P.A., and Samuel, A.D. (2015). Sensory determinants of
414 behavioral dynamics in Drosophila thermotaxis. Proceedings of the National Academy
415 of Sciences of the United States of America *112*, E220-229. doi:
416 10.1073/pnas.1416212112

417 Koh, T.W., He, Z., Gorur-Shandilya, S., Menuz, K., Larter, N.K., Stewart, S., and
418 Carlson, J.R. (2014). The Drosophila IR20a clade of ionotropic receptors are candidate
419 taste and pheromone receptors. Neuron *83*, 850-865. doi:
420 10.1016/j.neuron.2014.07.012

421 Liu, L., Li, Y., Wang, R., Yin, C., Dong, Q., Hing, H., Kim, C., and Welsh, M.J. (2007).
422 Drosophila hygrosensation requires the TRP channels water witch and nanchung.
423 Nature *450*, 294-298.

424 Mao, C.X., Xiong, Y., Xiong, Z., Wang, Q., Zhang, Y.Q., and Jin, S. (2014). Microtubule-
425 severing protein Katanin regulates neuromuscular junction development and dendritic
426 elaboration in Drosophila. Development *141*, 1064-1074. doi: 10.1242/dev.097774

427 Ni, L., Bronk, P., Chang, E.C., Lowell, A.M., Flam, J.O., Panzano, V.C., Theobald, D.L.,
428 Griffith, L.C., and Garrity, P.A. (2013). A gustatory receptor paralogue controls rapid
429 warmth avoidance in Drosophila. Nature *500*, 580-584. doi: 10.1038/nature12390

430 Ni, L., Klein, M., Svec, K.V., Budelli, G., Chang, E.C., Ferrer, A.J., Benton, R., Samuel,
431 A.D.T., and Garrity, P.A. (2016). The Ionotropic Receptors IR21a and IR25a mediate
432 cool sensing in *Drosophila*. eLife *5*, e13254. doi:
433 http://dx.doi.org/10.7554/eLife.13254.001

434 Olanga, E.A., Okal, M.N., Mbadi, P.A., Kokwaro, E.D., and Mukabana, W.R. (2010).
435 Attraction of Anopheles gambiae to odour baits augmented with heat and moisture.
436 Malaria journal *9*, 6. doi: 10.1186/1475-2875-9-6

437 Perttunen, V., and Salmi, H. (1956). The responses of Drosphila melanogaster Dipt.
438 Drosophilidae to the relative humidity of the air. Suomen hyonteistieteellinen
439 aikakauskirja: Annales entomologici Fennici *22*, 36-45.

Perttunen, V., and Syrjamaki, J. (1958). The effect of antennaectomy on the humidity reactions of Drosophila melanogaster. Suomen hyonteistieteellinen aikakauskirja: Annales entomologici Fennici *24*, 78-83.

Pfeiffer, B.D., Truman, J.W., and Rubin, G.M. (2012). Using translational enhancers to increase transgene expression in Drosophila. Proceedings of the National Academy of Sciences of the United States of America *109*, 6626-6631. doi: 10.1073/pnas.1204520109

Port, F., Chen, H.M., Lee, T., and Bullock, S.L. (2014). Optimized CRISPR/Cas tools for efficient germline and somatic genome engineering in Drosophila. Proceedings of the National Academy of Sciences of the United States of America *111*, E2967-2976. doi: 10.1073/pnas.1405500111

Russell, J., Vidal-Gadea, A.G., Makay, A., Lanam, C., and Pierce-Shimomura, J.T. (2014). Humidity sensation requires both mechanosensory and thermosensory pathways in Caenorhabditis elegans. Proceedings of the National Academy of Sciences of the United States of America *111*, 8269-8274. doi: 10.1073/pnas.1322512111

Rytz, R., Croset, V., and Benton, R. (2013). Ionotropic receptors (IRs): chemosensory ionotropic glutamate receptors in Drosophila and beyond. Insect biochemistry and molecular biology *43*, 888-897. doi: 10.1016/j.ibmb.2013.02.007

Saina, M., and Benton, R. (2013). Visualizing olfactory receptor expression and localization in Drosophila. Methods in molecular biology *1003*, 211-228. doi: 10.1007/978-1-62703-377-0_16

461 Sayeed, O., and Benzer, S. (1996). Behavioral genetics of thermosensation and
462 hygrosensation in Drosophila. Proceedings of the National Academy of Sciences of the
463 United States of America *93*, 6079-6084.

464 Shanbhag, S.R., Singh, K., and Singh, R.N. (1995). Fine structure and primary sensory
465 projections of sensilla located in the sacculus of the antenna of Drosophila
466 melanogaster. Cell and tissue research *282*, 237-249.

467 Silbering, A.F., Bell, R., Galizia, C.G., and Benton, R. (2012). Calcium imaging of odor-
468 evoked responses in the Drosophila antennal lobe. Journal of visualized experiments :
469 JoVE. doi: 10.3791/2976

470 Silbering, A.F., Bell, R., Münch, D., Cruchet, S., Gomez-Diaz, C., Laudes, T., Galizia,
471 C.G., and Benton, R. (2016). IR40a neurons are not DEET detectors. Nature *in press*.

472 Silbering, A.F., Rytz, R., Grosjean, Y., Abuin, L., Ramdya, P., Jefferis, G.S., and
473 Benton, R. (2011). Complementary function and integrated wiring of the evolutionarily
474 distinct Drosophila olfactory subsystems. J Neurosci *31*, 13357-13375. doi:
475 10.1523/JNEUROSCI.2360-11.2011

476 Stocker, R.F. (1994). The organization of the chemosensory system in Drosophila
477 melanogaster: a review. Cell and tissue research *275*, 3-26.

478 Thevenaz, P., Ruttimann, U.E., and Unser, M. (1998). A pyramid approach to subpixel
479 registration based on intensity. IEEE transactions on image processing : a publication of
480 the IEEE Signal Processing Society *7*, 27-41. doi: 10.1109/83.650848

481 Tichy, H., and Gingl, E. (2001). Problems in hygro- and thermoreception. In The ecology
482 of sensing, F.G. Barth, and A. Schimd, eds. (New York: Springer), pp. 271-287.

483 Tichy, H., and Kallina, W. (2010). Insect hygroreceptor responses to continuous
484 changes in humidity and air pressure. Journal of neurophysiology *103*, 3274-3286. doi:
485 10.1152/jn.01043.2009

486 Venken, K.J., Schulze, K.L., Haelterman, N.A., Pan, H., He, Y., Evans-Holm, M.,
487 Carlson, J.W., Levis, R.W., Spradling, A.C., Hoskins, R.A., and Bellen, H.J. (2011).
488 MiMIC: a highly versatile transposon insertion resource for engineering Drosophila
489 melanogaster genes. Nature methods *8*, 737-743.

490 Yao, C.A., Ignell, R., and Carlson, J.R. (2005). Chemosensory coding by neurons in the
491 coeloconic sensilla of the Drosophila antenna. J Neurosci *25*, 8359-8367. doi:
492 10.1523/JNEUROSCI.2432-05.2005

493 Zhang, Y.V., Ni, J., and Montell, C. (2013). The molecular basis for attractive salt-taste
494 coding in Drosophila. Science *340*, 1334-1338. doi: 10.1126/science.1234133
495

496

Figure 1

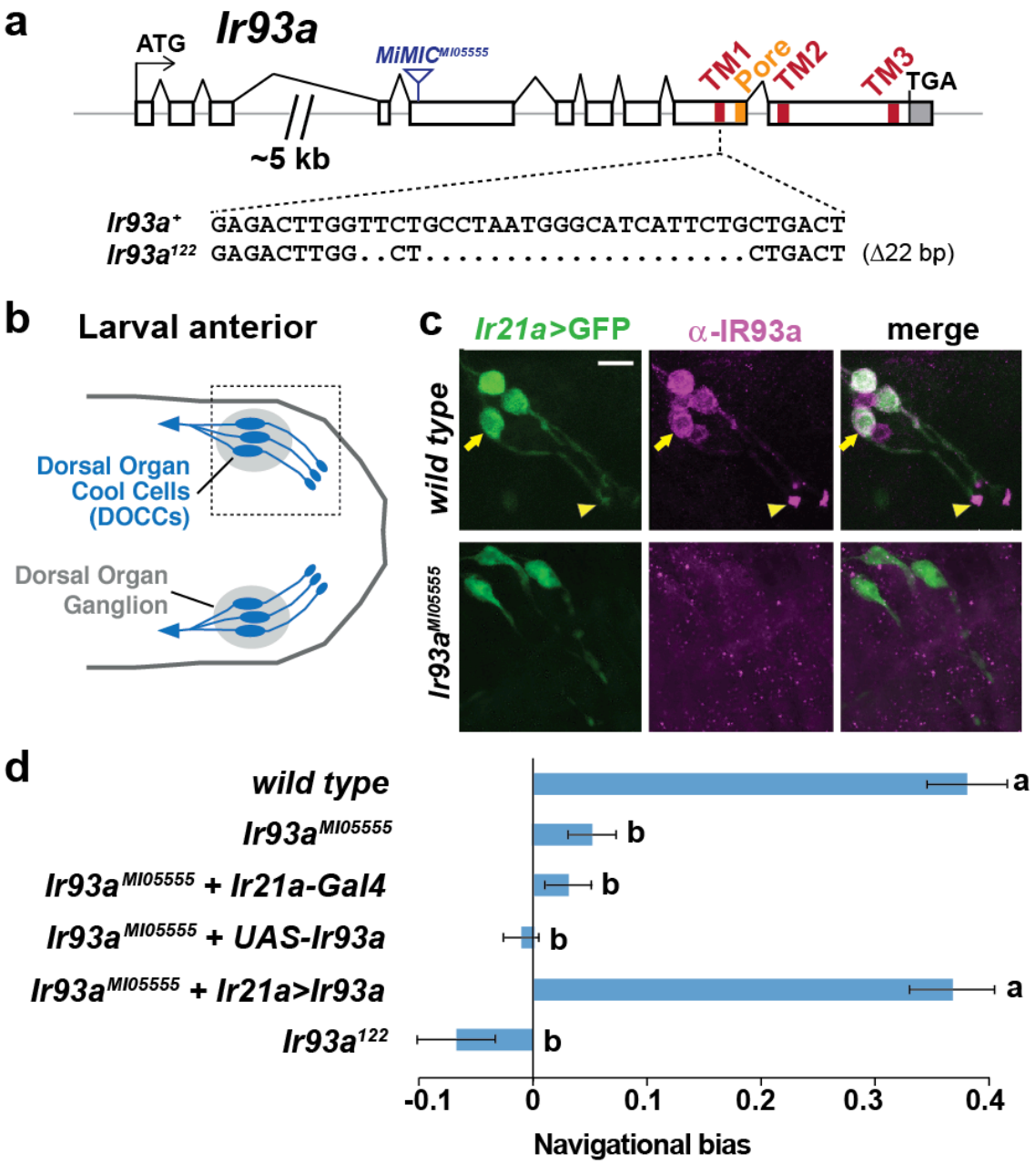

497
498

Figure 1. IR93a is expressed in Dorsal Organ Cool Cells (DOCCs) and is required for cool avoidance. (a) Gene structure of the *Ir93a* locus; sequences encoding the transmembrane (TM) domains and channel pore are colored. The blue triangle denotes site of *MiMIC* insertion in $Ir93a^{MI05555}$, and the CRISPR/Cas9-generated deletion in the $Ir93a^{134}$ allele is shown below. (b) Schematic of the larval anterior showing the bilaterally symmetric Dorsal Organ Ganglia (grey) within which three Dorsal Organ Cool Cells (DOCCs) are located. (c) Immunofluorescence of the larval anterior (corresponding to the boxed region in the schematic) showing expression of IR93a protein (magenta) in DOCCs (*Ir21a-Gal4;UAS-GFP* (*Ir21a>GFP*)) (green), as well as additional sensory neurons. $Ir93a^{MI05555}$ mutants lack IR93a immunostaining. The arrow and arrowhead label the soma and dendritic bulb of one of the DOCCs. Scale bar is 10 μm. (d) Cool avoidance behavior assessed as navigational bias (movement toward warmth / total path length) of individual larval trajectories on an ~0.36˚C/cm gradient extending from ~13.5˚C to ~21.5˚C, with a midpoint of ~17.5˚C. Letters denote statistically distinct categories (alpha=0.05; Tukey HSD). *wild type* (*Canton-S*), n=37 animals. $Ir93a^{MI05555}$, n=132. *Ir21a-Gal4/+;* $Ir93a^{MI05555}$, n=72. $Ir93a^{MI05555}$*,UAS-Ir93a/* $Ir93a^{MI05555}$*,+*, n=80. *Ir21a-Gal4/+;* $Ir93a^{MI05555}$*,UAS-Ir93a/* $Ir93a^{MI05555}$*,+*, n=45. $Ir93a^{122}$, n=101.

Figure 2

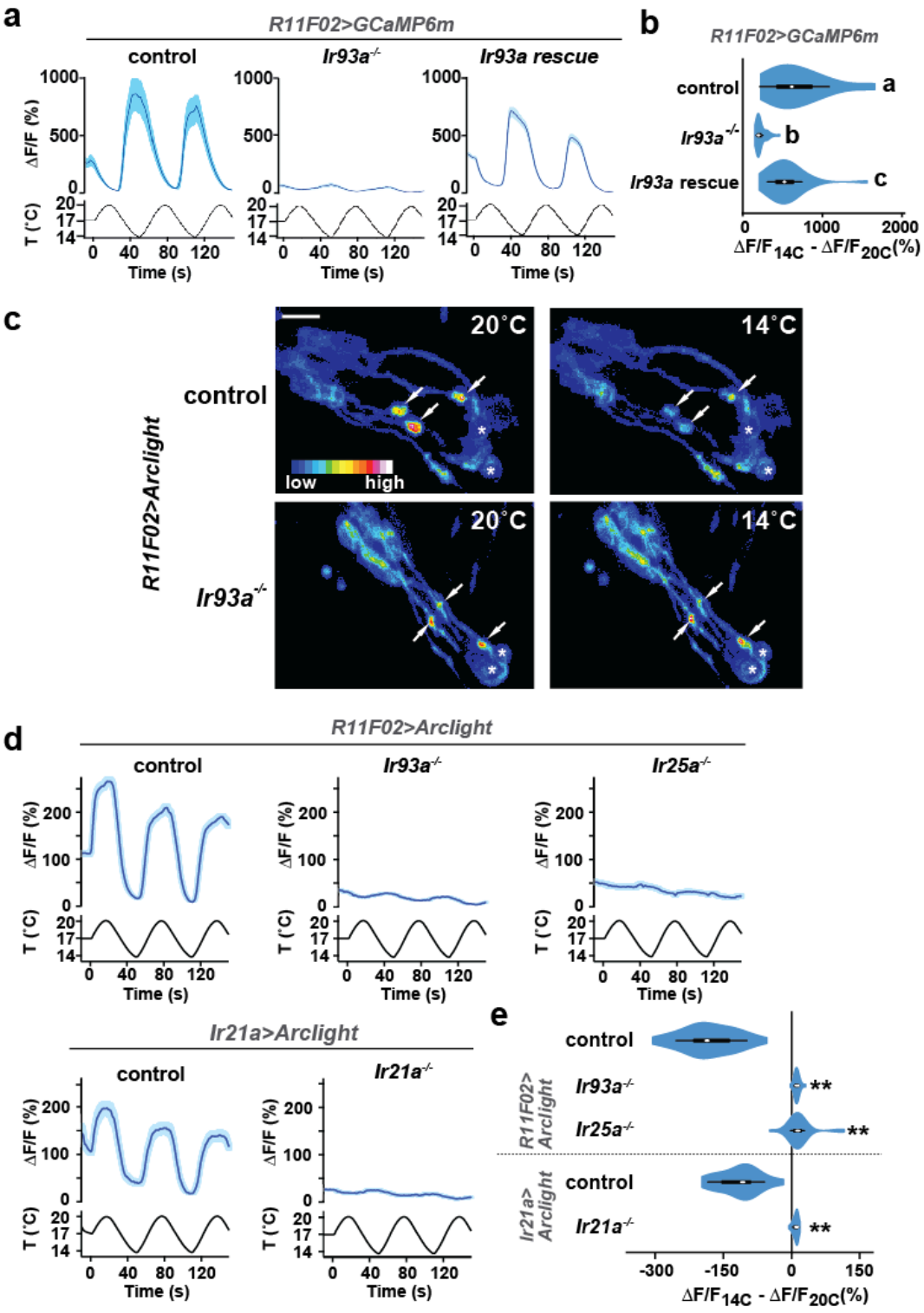

518
519

Figure 2: Cool-responsive calcium and voltage changes in DOCCs require IR93a.

(a) Left: DOCC responses monitored using *R11F02>GCaMP6m*. DOCC cool-responsive increases in fluorescence are dramatically reduced in *Ir93a*^{MI05555}, and responses are rescued by expression of a wild-type *Ir93a* cDNA under *R11F02-Gal4* control. Traces, average ± SEM. Right: Ratio of fluorescence at 14˚C versus 20˚C depicted using a violin plot (internal white circles show median; black boxes denote 25th to 75th percentiles; whiskers extend 1.5 times interquartile range). Letters denote statistically distinct categories, p<0.01, Steel-Dwass test. *wild type*, n=12 cells. *Ir93a*^{MI05555}, n=44. *Ir93a*^{MI05555}*; R11F02>Ir93a*, n=46. (b) Temperature-dependent DOCC voltage responses in the sensory endings of *wild-type* (upper panels) or *Ir93a*^{MI05555} mutant (lower panels) larvae monitored using *R11F02>Arclight*. Arrowheads denote DOCC dendritic bulbs. Note that Arclight fluorescence decreases upon depolarization. Asterisks denote cuticular autofluorescence from adjacent sensory structures. (c) Robust cool-responsive depolarization of DOCC sensory endings is observed in otherwise *wild-type* animals using either *R11F02>Arclight* or *Ir21a>Arclight*. Depolarization response is eliminated in *Ir93a*^{MI05555}, *Ir25a*^{2}, and *Ir21a*$^{\Delta 1}$ mutants. Traces, average ± SEM. Violin plot depicts ratio of fluorescence at 14˚C versus 20˚C. ** denotes distinct from wild-type control, p<0.01 compared to control, Steel-Dwass test. *R11F02-Gal4;UAS-Arclight*, n=57 cells. *R11F02-Gal4;UAS-Arclight*;*Ir93a*^{MI05555}, n=24. *R11F02-Gal4;UAS-Arclight*; *Ir25a*^{2}, n=30. *Ir21a-Gal4;UAS-Arclight*, n=18. *Ir21a-Gal4;UAS-Arclight*; *Ir21a*$^{\Delta 1}$, n=23.

Figure 3

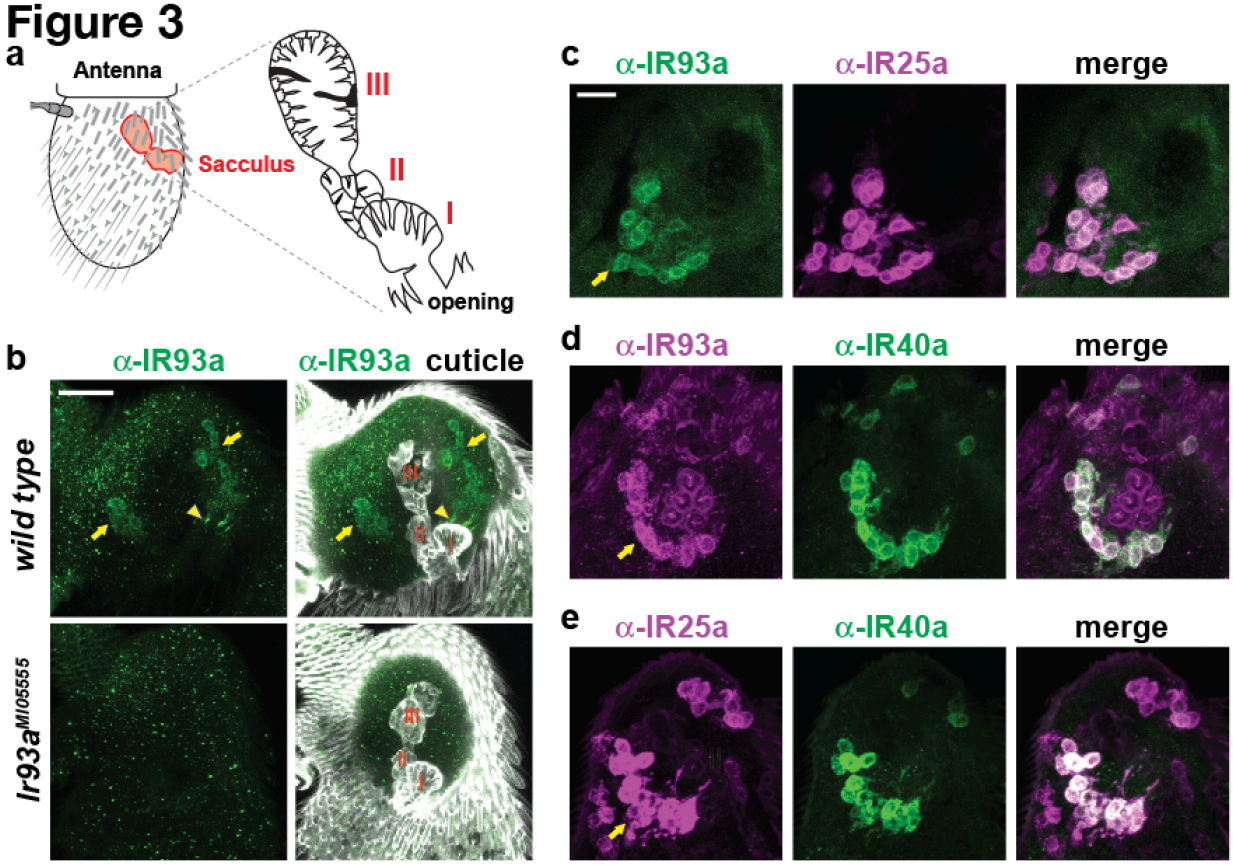

543

544

Figure 3: IR93a is co-expressed with IR25a and IR40a in sacculus neurons. (a) Left: schematic of the adult *Drosophila* antenna, illustrating the location of the sacculus (red) in the interior of this appendage. Right: the sacculus is composed of three main chambers (I, II, III), which are lined with sensilla of various morphologies (cartoon adapted from (Shanbhag et al., 1995)). (b) Top: immunofluorescence on a whole-mount wild-type antenna showing expression of IR93a protein (green) in two groups of soma (arrows) around sacculus chambers I and II; these chambers are visualized by cuticle autofluorescence shown in the images on the right. The arrowhead marks the concentration of IR93a in the dendritic endings that innervate the sensilla in chamber I. Note that the dendrites of chamber II neurons are no visible in this image; sensilla localization of IR93a is more easily detected in these cells in antennal sections; see panel (d). Bottom: *Ir93a*^{MI05555} mutants lack detectable IR93a protein. Scale bar is 20 μm**.** (c-e) Double immunofluorescence with the indicated antibodies on antennal cryosections revealing co-expression of these IRs in sacculus neurons; the arrows point to the cluster of neurons innervating chamber II. Scale bar is 10 μm. IR25a is expressed in additional neurons that do not express IR93a or IR40a because of IR25a's broader role as an olfactory IR co-receptor (Abuin et al., 2011).

Figure 4

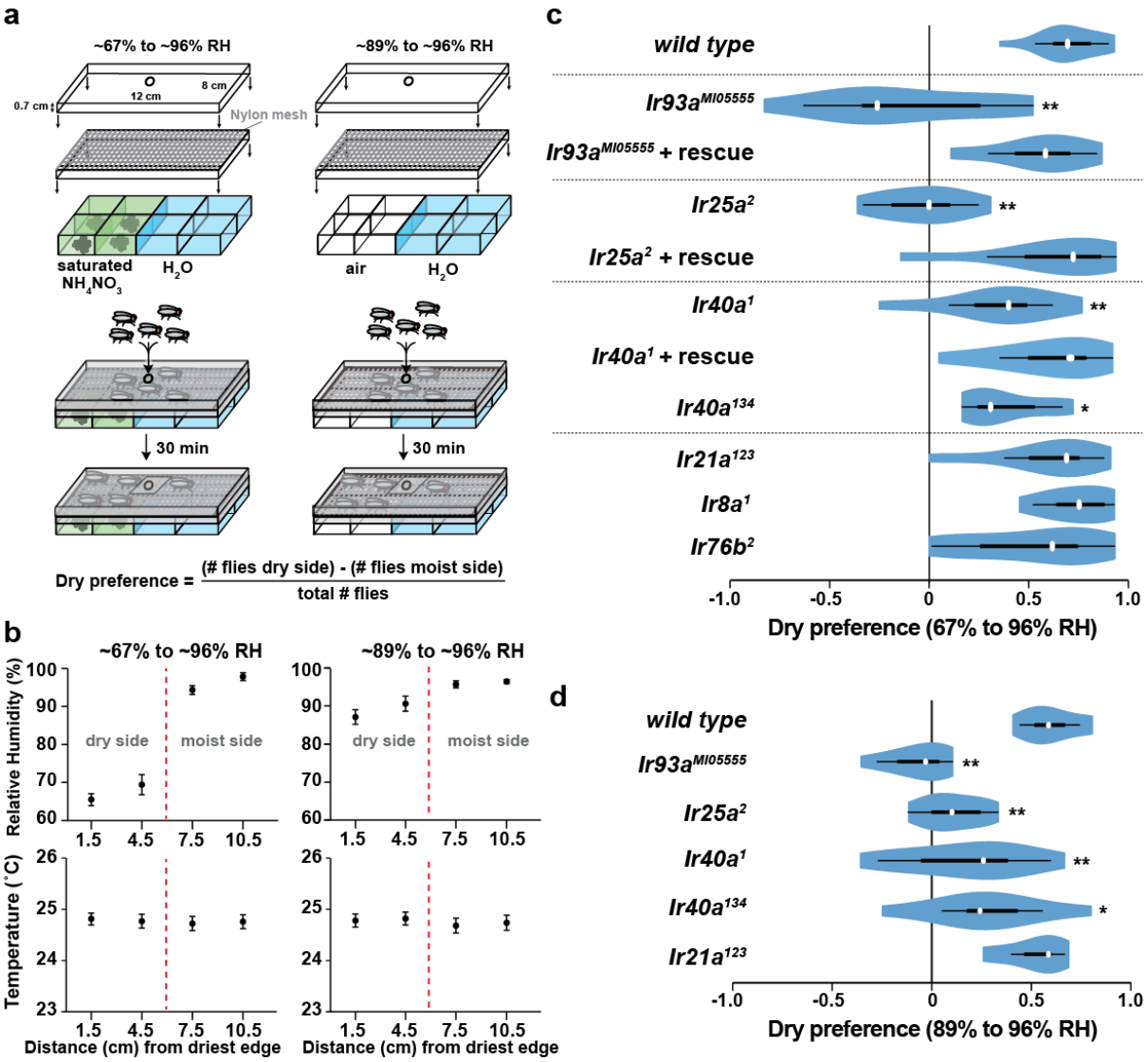

563

564

Figure 4: Hygrosensory behavior requires IR93a, IR25a and IR40a. (a) Schematic of the hygrosensory behavior assays. ~67% to ~96% RH gradients were generated by filling wells with either a saturated solution of ammonium nitrate in water and or pure water. ~89% to ~96% RH gradients were generated by pairing empty wells with wells filled with pure water. Nylon mesh prevented fly contact with solutions. Dry preference was quantified by counting flies on either side of chamber midline. 25-35 flies were used per assay. (b) Mean ± SD of RH and temperature measured at indicated gradient positions. ~67% to ~96% RH, n=58 gradients. ~89% to ~96% RH, n=28. (c,d) Dry preference assessed on ~67% vs. ~96% (c) and ~89% vs. ~96% (d) gradients. Asterisks denote statistically distinct from *wild type* (** p<0.01; * p<0.05, Steel with control). *wild type*, n=16 assays. *Ir8a* mutant ($Ir8a^{1}$), n=8. *Ir76b* mutant ($Ir76b^{2}$), n=14. *Ir21a* mutant ($Ir21a^{123}$), n=14. *Ir25a* mutant ($Ir26a^{2}$), n=11. Ir25a rescue ($Ir25a^{2}$; *UAS-*$Ir25a^{+}$), n=15. *Ir40a* mutant ($Ir40a^{1}$), n=15. *Ir40a* rescue ($Ir40a^{1}$; *UAS-*$Ir40a^{+}$), n=9. *Ir40a* CRISPR mutant ($Ir40a^{134}$), n=10. *Ir93a* mutant ($Ir93a^{MI05555}$), n=11. *Ir93a* rescue ($Ir93a^{MI05555}$, *UAS-*$Ir93a^{+}$), n=14. *Ir40a* mutant alleles and thermosensory behavior are shown in Figure 4 supplement 1a-b. Note that *UAS-cDNA* rescues were observed in the absence of *Gal4* drivers, reflecting *Gal4*-independent expression of *UAS* transgenes in the sacculus (Figure 4 supplement 1c).

Figure 4 - supplement 1

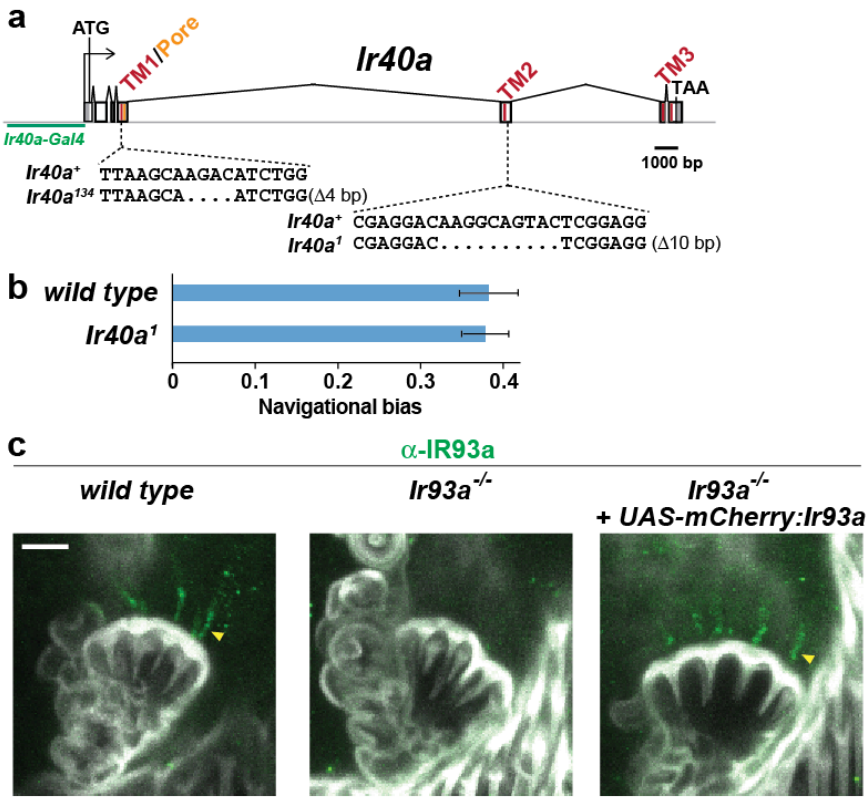

584

585 **Figure 4– Figure supplement 1:** (a) Gene structure and sequence alterations in *Ir40a*
586 alleles. Regions encoding transmembrane domains (TMs) and pore region are in red.
587 The *Ir40a* promoter region present in *Ir40a-Gal4* is indicated in green. (b) Larval cool
588 avoidance behavior (assayed as in Figure 1d) is unaffected by mutation of *Ir40a. wild*
589 *type*, n=37 animals. $Ir40a^{1}$, n=55. (c) IR93a protein expression in the sacculus of *wild-*
590 *type,* $Ir93a^{MI05555}$ and $Ir93a^{MI05555}$*;UAS-IR93a* animals. The *UAS-mCherry:IR93a*
591 transgene restores expression of IR93a protein in the dendrites of sacculus neurons
592 (arrowhead) without the need for a Gal4 driver. The reason for the Gal4-independent
593 expression in these neurons is unknown, but Gal4-independent expression of UAS
594 transgenes in specific cellular contexts has been previously reported (Mao et al., 2014).

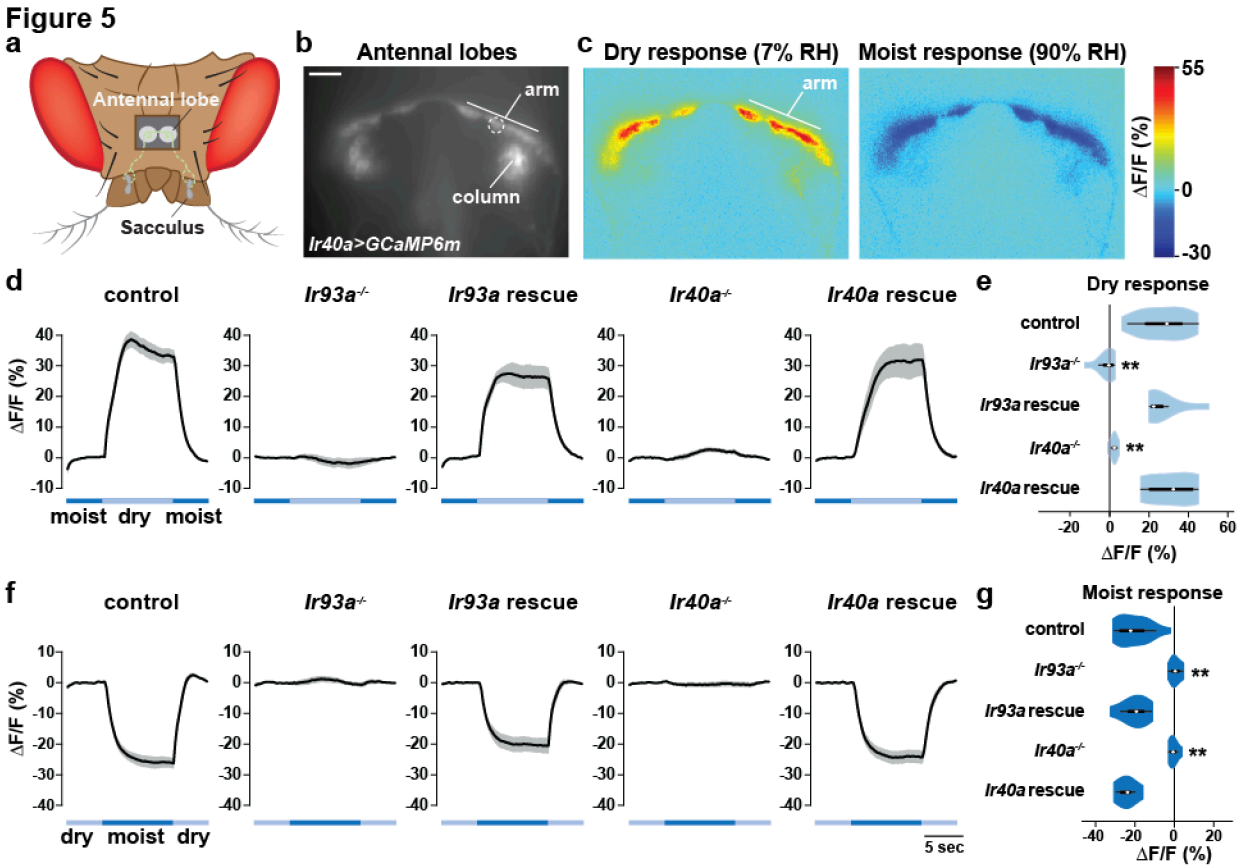

Figure 5: IR-dependent physiological responses to dry air. (a) Schematic of the *Drosophila* head (viewed from above) illustrating the projection of IR40a/IR93a/IR25a-expressing neurons (green) (labeled using *Ir40a-Gal4* (Silbering et al., 2011)) from the sacculus to the antennal lobes in the brain, visualized through a hole in the head cuticle. (b) Raw fluorescence image of *Ir40a* axons (in *Ir40a-Gal4;UAS-GCaMP6m* animals) innervating the arm and column in the antennal lobe. The dashed circle indicates the position of the ROI used for quantification in panels (d-g). (c) Color-coded images (reflecting GCaMP6m fluorescence intensity changes) of IR40a neuron responses to a switch from 90% to 7% RH ("Dry response") and to a switch from 7% to 90% RH ("Moist response"). (d, f) Moisture-responsive fluorescence changes in the arm (moist=90% RH, dry=7% RH). Traces represent average ±SEM. (e, g) Quantification of changes in ΔF/F

(mean fluorescence change in the ROI shown in (b)) upon shift from moist to dry (e) or dry to moist (g). Dry responses were quantified as [ΔF/F at 7% RH (average from 4.5 to 6.5 s after shift to 7% RH)] - [ΔF/F at 90% RH (average from 3.5 to 1 s prior to shift to 7% RH)], and moist responses quantified by performing the converse calculation. Genotypes: control: n=17 animals (pooled data from *Ir40a-Gal4,Ir40a*^{1}*/IR40a-Gal4,+;UAS-GCaMP6m/+,* n=9; *IR40a-Gal4;UAS-GCaMP6m,Ir93a*^{MI05555}/+, n=8). *Ir93a* mutant (*Ir40a-Gal4;UAS-GCaMP6m,Ir93a*^{MI05555}*/Ir93a*^{MI05555}*)*, n=10. *Ir93a* rescue (*Ir40a-Gal4;UAS-GCaMP6m,Ir93a*^{MI05555}*/UAS-mcherry:Ir93a,Ir93a*^{MI05555}*)*, n=8. *Ir40a* mutant *(Ir40a-Gal4,Ir40a*^{1}*;UAS-GCaMP6m/+)*, n=8. *Ir40a* rescue (*Ir40a-Gal4,Ir40a*^{1}*;UAS-GCaMP6m/UAS-Ir40a)*, n=6. **p<0.01, distinct from controls and rescues, Steel-Dwass test.